Comparative study on transient stability analysis of wind turbine generator system using different drive train models

S.M. Muyeen, Md. Hasan Ali, R. Takahashi, T. Murata, J. Tamura, Y. Tomaki, A. Sakahara and E. Sasano

Abstract: A huge number of wind generators are going to be connected with the existing network in the near future. Therefore it is necessary to analyse the transient stability of power systems, including wind turbine generator systems (WTGS). It has already been reported that one-mass or lumped model of wind turbine system is insufficient to analyse the transient behaviour of WTGS. It has also been reported that for the precise transient analysis of WTGS, a six-mass drive train model is needed. The reduced order models (three-mass and two-mass) have also been adopted so far for transient behaviour analysis. But the transient stability analysis of using six-mass, three-mass and two-mass drive train models has not been reported sufficiently so far in the literature. The authors have conducted an analysis using these methods. First, a detailed transformation procedure is presented from six-mass drive train model to two-mass model, which can be used in the analysis of transient stability simulation with sufficient accuracy. It is then determined which drive train model is appropriate for transient stability analysis of grid-connected WTGS. The effects of drive train parameters (such as inertia constant, spring constant and damping constant) on stability are examined using the above mentioned types of drive train models. Moreover, different types of symmetrical and asymmetrical faults at different wind generator power levels are considered in the simulation analyses with and without considering damping constants in six-mass, three-mass and two-mass shaft models. Considering the simulation results, it can be concluded that two-mass shaft model is sufficient for the transient stability analysis of WTGS.

List of symbols

ρ	air density
R	turbine blade radius
V_w	wind speed
C_p	power coefficient
λ	tip speed ratio
β	blade pitch angle
P_w	extracted power from the wind
ω_B	hub angular velocity
ω_{GB}	gearbox angular velocity
ω_G	generator angular velocity
θ_B	hub angular position
θ_{GB}	gearbox angular position
θ_G	generator angular position
J	mass moment of inertia
M	weight of the disk
L	length of the shaft
G	shear modulus
D_d	diameter of the disk
D_{sh}	shaft diameter
H_B	hub inertia constant
H_{GB}	gearbox inertia constant
H_G	generator inertia constant
K_{HB}	spring constant between hub and blade
K_{HGB}	spring constant between hub and gearbox
K_{GBG}	spring constant between gearbox and generator
K_{2M}	spring constant of the shaft in two-mass model
D	self-damping of individual masses
d	mutual damping of adjacent masses
T_e	electromagnetic torque of induction generator
T_B	torque acting on blade
N_{GB}	gear ratio
CB	circuit breaker
r_a	armature resistance
x_a	armature reactance
X_d	direct-axis synchronous reactance
X_q	quadrature-axis synchronous reactance
X'_d	direct-axis transient reactance
X'_q	quadrature-axis transient reactance
X''_d	direct-axis subtransient reactance
X''_q	quadrature-axis subtransient reactance

doi:10.1049/iet-rpg:20060030

Paper first received 22nd December 2006 and in revised form 26th March 2007

S.M. Muyeen, R. Takahashi, T. Murata and J. Tamura are with the Department of EEE, Kitami Institute of Technology, 165 Koen-cho, Kitami 090-8507, Japan

Md. Hasan Ali is with the Changwon National University, 9 Sarim-Dong, Changwon, Gyeongnam 641-773, South Korea

Y. Tomaki, A. Sakahara and E. Sasano are with the Hokkaido Electric Power Co., Inc., Sapporo 060-8677, Japan

E-mail: muyeen0809@yahoo.com

T'_{q0}	direct-axis open circuit transient time constant
T''_{d}	direct-axis open circuit subtransient time constant
T''_{q0}	quadrature-axis open circuit subtransient time constant
r_1	stator resistance
x_1	stator unsaturated leakage reactance
X_{mu}	unsaturated magnetising reactance
r_{21}	first cage resistance
x_{21}	rotor unsaturated mutual reactance
r_{22}	second cage resistance
x_{22}	second cage unsaturated reactance
SG	synchronous generator
SG_{δ}	load angle of synchronous generator
IG	induction generator

1 Introduction

Electrical energy generation using wind power has recently received considerable interest and attention all over the world due to growing environmental concern [1]. A huge number of wind farms are going to be connected with the existing network in the near future. Induction generators (IGs) are generally used as wind generators because of their superior characteristics such as brushless and rugged construction, low cost, low maintenance and simple operation. But as IG has stability problems such as the transient stability of synchronous generators (SG) [2], it is essential to investigate the transient stability of power systems including wind generators. There are several reports investigating the transient stability of wind generators in fault conditions [3–7]. In these references however, wind turbines and wind generators are modelled as a one-mass lumped model with a combined inertia constant.

Although the one-mass lumped model is too simple for representing the dynamics of a wind turbine and wind generator connected to each other through a shaft, stability analysis based on the one-mass shaft model may give significant errors. Wind turbine generator system (WTGS) is the only generator unit in a utility network where mechanical stiffness is lower than electrical stiffness (synchronising torque coefficient) [8]. Moreover, inertia constants of the turbine and generator have significant effects on the transient stability. Valuable studies have been performed for transient stability, fault analysis, reactive power compensation and other simulation analyses of WTGS by using two-mass shaft model [8–18]. For example, studies for fault-clearing time by using a two-mass shaft model were presented in [16–18]. In other studies [19–25], three-mass or higher order shaft models were also analysed. Flicker and power fluctuation analyses were discussed in [15, 23], where multi-mass shaft model was considered. The torsional natural frequency of wind generators was discussed in [7, 15, 23], where a multi-mass shaft model was also considered. But from these reports, the characteristic accuracy of each WTGS model, namely six-mass, three-mass and two-mass drive train models, cannot be cleared. To clear the characteristics between the six-mass model and reduced order models (three- and two-mass drive train models), proper definitions of all concepts under comparison must first be made. Next, all concepts under consideration should have parameters that can be obtained using the proper transformation technique from a base parameter set of a six-mass drive train model, which is considered as a benchmark model in this study. Finally, all concepts under consideration should be compared to each other under exactly the same operating conditions. In our previous work [9], we stated that the two-mass shaft model rather than one-mass lumped model should be used for transient stability analysis because the stiffness and inertia constant of wind turbine shaft systems have a great effect on the transient stability. In [19], the transient stability of WTGS was analysed using only two-mass and three-mass models, where the transformation from a three-mass to two-mass drive train model was not confirmed by simulation results and moreover, all types of damping effects were disregarded. But in the relevant study [25], it was found that the transient stability analysis without considering damping effects can give pessimistic results and thus it was concluded that for precise transient stability analysis, the six-mass drive train model is the right choice. However, six-mass drive train modelling slows the simulations due to complex and lengthy mathematical computation with small time-steps. This study attempts to compare the results of different types of drive train models of WTGS for transient stability analysis. It will be shown that the reduced order two-mass shaft model is acceptable for transient stability analysis of WTGS.

As wind speed is intermittent and stochastic in nature, the torques acting on blades of wind turbines are not always equal. Only with the six-mass drive train model can this unequal blade torque sharing can be analysed. In this work, it is ensured that the unequal blade torque distributions have no effect on the transient stability of WTGS, which encourages the consideration of the reduced order three-mass and two-mass models. The six-mass drive train model parameters are referred to as the base parameter set. First, the three different model systems are described. Then the detailed transformation procedure from six-mass to two-mass drive train models is discussed, where self- and mutual-dampings are also considered. The validity of the transformation is confirmed by the simulation results, which is one of the novel features of this work. The effects of parameters such as spring constants, inertia constants and damping constants of six-mass, three-mass, and two-mass models on the transient stability of WTGS are investigated clearly. Different types of symmetrical and asymmetrical faults are analysed under different wind generator power conditions with and without considering damping constants of six-mass, three-mass and two-mass drive train models. Moreover, the simulation analyses are performed using two types of power system models for short and long duration network faults. From all the simulation results it is concluded that the two-mass shaft model is sufficient enough for the transient stability analysis of WTGS.

2 Wind turbine modelling

The mathematical relation for the mechanical power extracted from the wind can be expressed as follows [26]

$$P_w = 0.5\rho\pi R^2 v_w^3 C_p(\lambda, \beta) \qquad (1)$$

where P_w is the extracted power from the wind, ρ is the air density [kg/m^3], R is blade radius [m], V_w is wind speed [m/s] and C_p is the power coefficient, which is a function of both tip speed ratio, λ, and blade pitch angle, β [deg]. In this work, the C_p equation as shown below has been taken from [27].

$$\lambda = \frac{\omega_{\mathrm{H}} R}{V_{\mathrm{w}}} \tag{2a}$$

$$C_{\mathrm{p}} = \frac{1}{2}(\lambda - 0.022\beta^2 - 5.6)\mathrm{e}^{-0.17\lambda} \tag{2b}$$

where ω_{H} is the rotational speed of the hub [rad/s]. The C_{p}–λ curves are shown in Fig. 1 for different values of β.

Wind turbine torque, T_{wt}, can be expressed simply as follows

$$T_{\mathrm{wt}} = P_{\mathrm{w}}/\omega_{\mathrm{H}} \tag{3}$$

The detailed modelling of each drive train model and the conversion process from six-mass to two-mass shaft model are discussed next.

2.1 Six-mass drive train model

The basic six-mass drive train model is presented in Fig. 2*a*. The six-mass model system has six inertias, namely three blade inertias (H_{B1}, H_{B2} and H_{B3}), hub inertia (H_{H}), gearbox inertia (H_{GB}) and generator inertia (H_{G}). θ_{B1}, θ_{B2}, θ_{B3}, θ_{H}, θ_{GB} and θ_{G} represent angular velocities of the blades, hub, gearbox and generator; ω ω_{B1}, ω_{B2}, ω_{B3}, ω_{H}, ω_{GB} and ω_{G} correspond to angular positions of the blades, hub, gearbox and generator. The elasticity between adjacent masses is expressed by the spring constants K_{HB1}, K_{HB2}, K_{HB3}, K_{HGB} and K_{GBG}. The mutual-damping between adjacent masses is expressed by d_{HB1}, d_{HB2}, d_{HB3}, d_{HGB} and d_{GBG}. There exist some torque losses through external damping elements of individual masses, which are represented by D_{B1}, D_{B2}, D_{B3}, D_{H}, D_{GB} and D_{G}. The model system needs generator torque (T_{e}) and three individual aerodynamic torques acting on each blade (T_{B1}, T_{B2}, T_{B3}). The sum of the blade torques develops the turbine torque, T_{wt}. It is assumed that the aerodynamic torques acting on hub and gearbox are zero.

2.2 Three-mass drive train model

The basic three-mass model is shown in Fig. 2*b*. The turbine inertia can be calculated from the combined weight of three blades and hub. Therefore the mutual-damping between hub and blades is ignored in the three-mass model. Individual blade torque sharing cannot be considered in this model. Instead it is assumed that the three-blade turbine has uniform weight distribution for simplicity – that is, turbine torque, T_{wt}, is assumed to be equal to the summation of the torque acting on three blades. Therefore the turbine can be assumed as a large disk with small thickness. If proper data is not available, the simple equation below

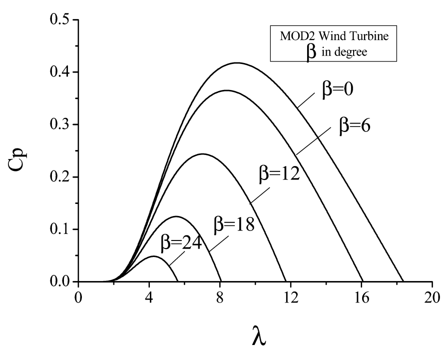

Fig. 1 *C_p–λ curves for different pitch angles*

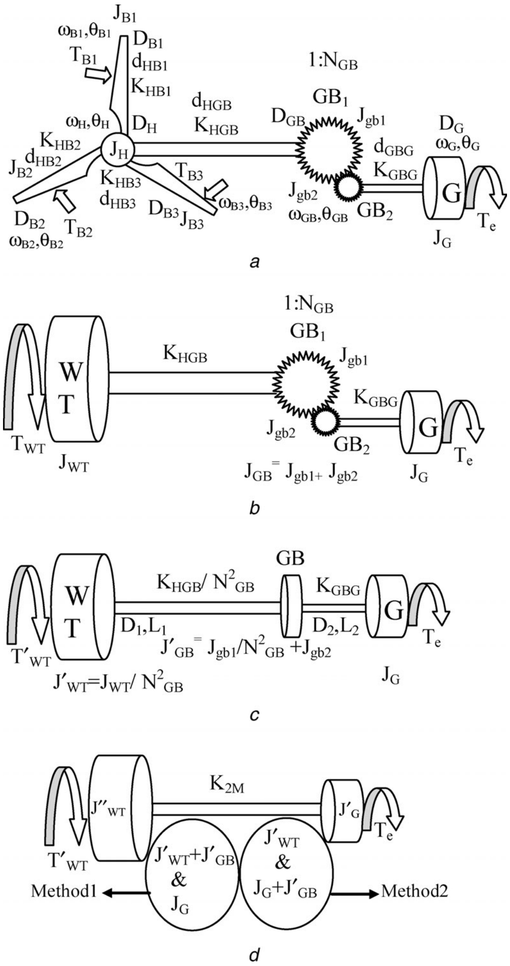

Fig. 2 *Drive train models of wind turbine generator system*

a Six-mass model
b Three-mass model
c Transformed three-mass system
d Two-mass model

can be used for the estimation of the mass moment of inertia of a disk with small thickness [28]

$$J(\mathrm{kg\ m^2}) = \frac{MD_{\mathrm{d}}^2}{8} \tag{4}$$

where D_{d} is diameter of the disc and M is weight of the disc. Similarly, generator and gearbox inertia can be calculated approximately from their diameter and weight. If we need precise estimations, precise data of geometry and very complicated formula are needed for calculating the moment of inertia of turbine, gearbox and generator.

The shaft stiffness can be calculated from the equation below [29]

$$K(\mathrm{Nm/rad}) = \frac{G\pi D_{\mathrm{sh}}^4}{32L} \tag{5}$$

where D_{sh} is shaft diameter, L is shaft length and G is shear modulus. Stainless steel or ductile cast iron is normally used as shaft material.

2.3 Geared system transformation

When the torsional system is interconnected by a set of gears, the inertia discs are not being operated at the same angular speed throughout the system. In such case, the actual system needs to be corrected for the differences in speed of the component parts – that is the inertias and spring constants are referred to one speed of rotation as shown in Fig. 2*c*. The basis for these transformations is that the potential and kinetic energies of the equivalent system should be the same as those of the actual one, and it is assumed that the gear teeth do not break contact while transmitting vibration. The above-mentioned transformation can be summarised as follows [29, 30]

$$\frac{J_{\mathrm{eq}}}{J_{\mathrm{a}}} = \frac{K_{\mathrm{eq}}}{K_{\mathrm{a}}} = (\text{Speed ratio})^2 \tag{6}$$

where the suffix 'eq' and 'a' means equivalent and actual, respectively.

2.4 Two-mass shaft model

The three-mass system can be converted into a two-mass system (as shown in Fig. 2*d*) by adding the masses of two discs together and by connecting the two discs with equivalent shaft stiffness. The equivalent shaft stiffness of the two-mass system, $K_{2\mathrm{M}}$, can be determined from the parallel shaft stiffness as in (7) [29, 30]. In Fig. 2*d*, J''_{wt} and J'_{G} represent the equivalent mass moment of inertia of wind turbine and generator, respectively. It should be mentioned that two discs should be added into one by considering the lower shaft stiffness. For example, if the spring constant of the low-speed side is lower than that of the high-speed side, then the gearbox and generator inertias should be added as shown in method 2 of Fig. 2*d* and vice versa, which can be confirmed by the simulation results presented in Section 5.1.1. This might be a good practice for wind turbine drive train conversion methodology instead of the conventional one of connecting turbine and gearbox together as presented in [18, 19]. Accordingly, the self-dampings of generator and gearbox should be added together and the mutual damping of gearbox and generator is neglected in two-mass shaft model.

$$\frac{1}{K_{2\mathrm{M}}} = \frac{1}{(K_{\mathrm{HGB}}/N_{\mathrm{GB}}^2)} + \frac{1}{K_{\mathrm{GBG}}} \tag{7}$$

2.5 Per unitisation

In the drive train model system, all data used in the stated equations are converted to per unit system. If P_{B} is the base power (VA), ω_0 the base electrical angular velocity (rad/s) and P the number of pole pairs of the generator, the base values of the per unit system at the high-speed side of the drive train are defined as follows:

- The base mechanical speed (mech. rad/s) is $\omega'_{\mathrm{B}} = \omega_0/P$.
- The base torque (Nm) is $T'_{\mathrm{B}} = P_{\mathrm{B}}/\omega'_{\mathrm{B}}$.
- The base inertia (Nm/(rad/s)) is $J'_{\mathrm{B}} = T'_{\mathrm{B}}/0.5\omega'_{\mathrm{B}} = P_{\mathrm{B}}/0.5\omega'^2_{\mathrm{B}}$.
- The base spring constant (Nm/(rad/s)) is $K'_{\mathrm{B}} = T'_{\mathrm{B}}/\omega'_{\mathrm{B}} = P_{\mathrm{B}}/\omega'^2_{\mathrm{B}}$.
- The base damping constant (Nm/(rad/s)) is $D'_{\mathrm{B}} = d'_{\mathrm{B}} = T_{\mathrm{B}}/\omega'_{\mathrm{B}} = P_{\mathrm{B}}/\omega'^2_{\mathrm{B}}$.

Now, the low-speed side (turbine-side) base quantities can be calculated from the high-speed side (generator-side) base quantities using the gearbox speed ratio, N_{GB}, as follows

$$\begin{aligned} \omega''_{\mathrm{B}} &= \omega'_{\mathrm{B}}/N_{\mathrm{GB}} \quad & J''_{\mathrm{B}} &= N_{\mathrm{GB}}^2 J'_{\mathrm{B}} \\ \theta''_{\mathrm{B}} &= \theta'_{\mathrm{B}}/N_{\mathrm{GB}} \quad & D''_{\mathrm{B}} &= N_{\mathrm{GB}}^2 D'_{\mathrm{B}} \\ T''_{\mathrm{B}} &= N_{\mathrm{GB}} T'_{\mathrm{B}} \quad & K''_{\mathrm{B}} &= N_{\mathrm{GB}}^2 K'_{\mathrm{B}} \end{aligned} \tag{8}$$

In this paper, $H_{\mathrm{B}\,(1,2,3)}$, H_{H}, H_{GB} and H_{G} represent the per unit inertia constants (s) of three blades, hub, gearbox and generator, respectively.

2.6 Wind farm equivalent N-machine

For transient stability of WTGS it is cumbersome to simulate each individual wind turbine. So, wind turbines with same torsional natural frequency might be added as follows [5, 20]

$$\begin{aligned} J_{\mathrm{wt}} &= \sum_{i=1}^{p} J_{\mathrm{wt}i}; \quad J_{\mathrm{gb}} = \sum_{i=1}^{p} J_{\mathrm{gb}i}; \\ J_{\mathrm{g}} &= \sum_{i=1}^{p} J_{\mathrm{g}i}; \quad K = \sum_{i=1}^{p} K_i \end{aligned} \tag{9}$$

where i is the number of each individual wind turbine and p is the total number of wind turbine.

3 Simulation model

Two types of model systems are used for the sake of exact comparison among different types of drive train models of WTGS during network disturbances. Fig. 3 shows model system-I, where one SG is connected to an infinite bus through a transformer and a double circuit transmission line. In the figure, the double circuit transmission line parameters are numerically shown in the form of $R + jX$, where R and X represent the resistance and reactance, respectively. One wind farm (IG) is connected with the network via a transformer and short transmission line. A capacitor bank has been used for reactive power compensation at steady-state. The value of capacitor C is chosen so that the power factor of the wind power station becomes united [7] during the rated operation. Automatic voltage regulator and Governor control system models shown in Figs. 4 and 5, respectively, have been included in the SG model. Fig. 6 shows model system-II, where the aggregated model of wind farm (IG) is directly connected to the SG through a double circuit transmission line. The IEEE generic turbine model and approximate mechanical-hydraulic speed governing system is used with SG [31]. IEEE alternator supplied rectifier excitation system (AC1A) [32] is used for excitation control of SG. The generator parameters for both model systems are shown in Table 1. The initial values used for model systems I and II are shown in Tables 2 and 3, respectively. The drive

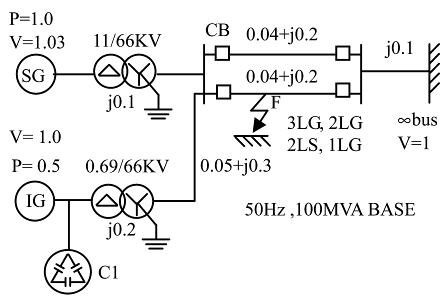

Fig. 3 *Model system-I*

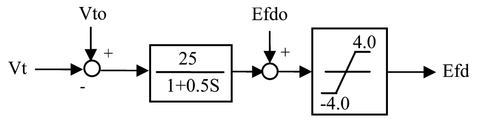

Fig. 4 *Automatic voltage regulator model*

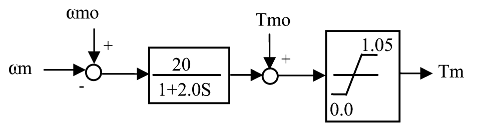

Fig. 5 *Governor model*

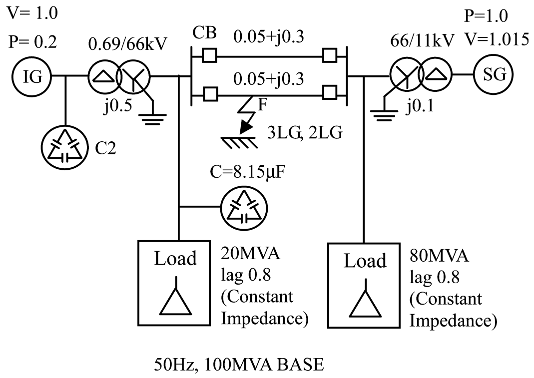

Fig. 6 *Model system-II*

Table 1: Generator parameters

SG		IG	
MVA	100	MVA	50/20
r_a (pu)	0.003	r_1 (pu)	0.01
x_a (pu)	0.13	x_1 (pu)	0.1
X_d (pu)	1.2	X_{mu} (pu)	3.5
X_q (pu)	0.7	r_{21} (pu)	0.035
X'_d (pu)	0.3	x_{21} (pu)	0.030
X'_q (pu)	0.22	r_{22} (pu)	0.014
X''_d (pu)	0.22	x_{22} (pu)	0.098
X''_q (pu)	0.25		
T'_{d_0} (s)	5.0		
T''_{d_0} (s)	0.04		
T''_{q_0} (s)	0.05		
H (s)	2.5		

Table 3: Initial conditions of generators and turbines (model system-II)

	Condition 4		Condition 5	
	SG	IG	SG	IG
P (pu)	0.624	0.16	0.58	0.20
V (pu)	1.015	1.014	1.015	1.00
Q (pu)	0.279	0.018 (0.081)[a]	0.297	0.000 (0.095)[a]
E_{fd} (pu)	1.50	–	1.50	–
T_m (pu)	0.626	–	0.582	–
Slip	0.0	−0.835%	0.0	−1.09%
V_w (m/s)	–	10.74	–	11.79
β (deg)	–	0	–	0

[a]Reactive power drawn by induction generator

train parameters for the six-mass, three-mass and two-mass models are shown in Section 10. For transient stability analysis the symmetrical three line-to-ground fault (3LG) is considered. Some unsymmetrical faults such as double line-to-ground fault (2LG) (phase a and b), double line-to-line fault (2LS) (between phase a and b) and single line-to-ground fault (1LG) (phase a) are also considered. Time step and simulation time have been chosen 0.00005 and 10 s, respectively. The simulations have been done by using PSCAD/EMTDC [33].

4 Effects of equal and unequal blade torque sharing on the stability

Wind speed is intermittent and stochastic in nature. Therefore, the torques acting on three blades of a wind turbine are not always equal. In this section, the effect of equal and unequal torque sharing on the transient stability are analysed by using the six-mass drive train model. A 3LG fault is considered to occur at fault point F of model system-I. The initial values for stable and unstable cases are shown as condition 1 and condition 2 in Table 2. The drive train parameters of six-mass model are shown in Section 10, but all types of dampings are disregarded in this case for considering the worst-case scenario. Responses of the IG rotor and turbine hub speeds are shown in Figs. 7 and 8, respectively, for both stable and unstable situations. It is seen from Figs. 7 and 8 that unequal blade torque sharing has no effect on the transient stability of WTGS. Therefore the three-mass and two-mass reduced order drive train models can be used, where it is assumed that the turbine torque is equal to the summation

Table 2: Initial conditions of generators and turbines (model system-I)

	Condition 1		Condition 2		Condition 3	
	SG	IG	SG	IG	SG	IG
P (pu)	1.0	0.39	1.0	0.40	1.0	0.50
V (pu)	1.03	1.042	1.03	1.039	1.03	0.999
Q (pu)	0.244	0.053 (0.206)[a]	0.251	0.049 (0.209)[a]	0.334	0.000 (0.239)[a]
E_{fd} (pu)	1.719	–	1.725	–	1.803	–
T_m (pu)	1.003	–	1.003	–	1.003	–
SG_δ (deg)	50.47	–	50.50	–	50.72	–
Slip	0.0	−0.769%	0.0	−0.794%	0.0	−1.09%
V_w (m/s)	–	10.615	–	10.722	–	11.797
β (deg)	–	0	–	0	–	0

[a]Reactive power drawn by induction generator

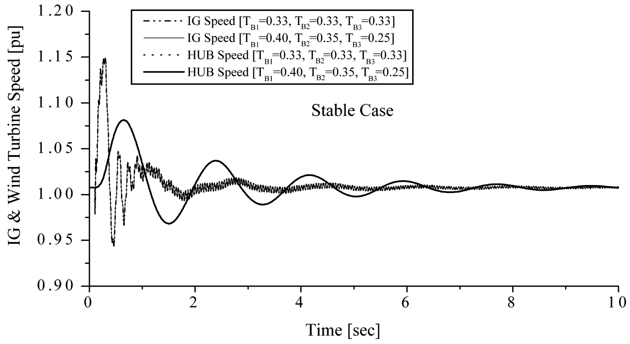

Fig. 7 *Transient effect of equal and unequal blade torque sharing (condition 1, 3LG, stable case, model system-I)*

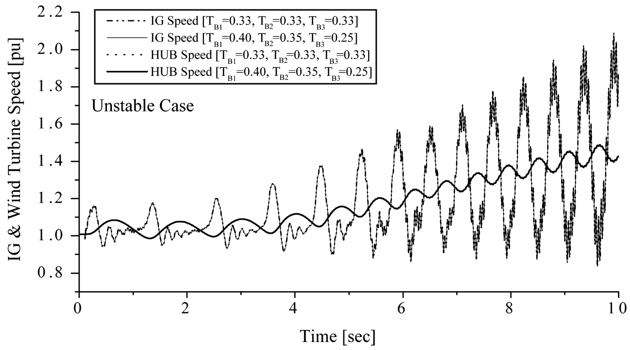

Fig. 8 *Transient effect of equal and unequal blade torque sharing (condition 2, 3LG, unstable case, model system-I)*

of the torques acting on the three-blades. The comparison between the three types of drive train models of WTGS during the network disturbances has been presented in Section 5 by using model systems I and II.

5 Comparison using model system-I

First, the effects of drive train parameters of the six-, three- and two-mass drive train models on the transient stability of WTGS are analysed by using model system-I. Then the comparison is also carried out at different IG output power levels for different types of symmetrical and asymmetrical faults. The fault is considered to occur at 0.1 s. The circuit breakers (CB) on the faulty line are opened at 0.2 s and the CBs are reclosed at 1.0 s.

5.1 Effects of drive train parameters on transient stability of WTGS

The effects of drive train parameters on the transient stability of grid connected WTGS are analysed by considering that the severe 3LG fault has occurred at point F of Fig. 3. The initial values are presented as condition 2 in Table 2.

5.1.1 Effect of inertia constants: In this sub-section, the effects of inertia constant on the transient stability of WTGS are analysed using six-mass, three-mass and two-mass drive train models. All types of dampings are neglected in this case. For the two-mass shaft model, two types of inertia sets are used as shown in Fig. 2*d*. Responses of the IG speed and turbine speed are shown in Figs. 9 and 10, respectively, for six-mass, three-mass and two-mass drive train models. Some other simulation results of IG rotor and turbine speeds are presented in Figs. 11 and 12, respectively, where the turbine inertia of each drive train model is increased by 50% from the original value shown

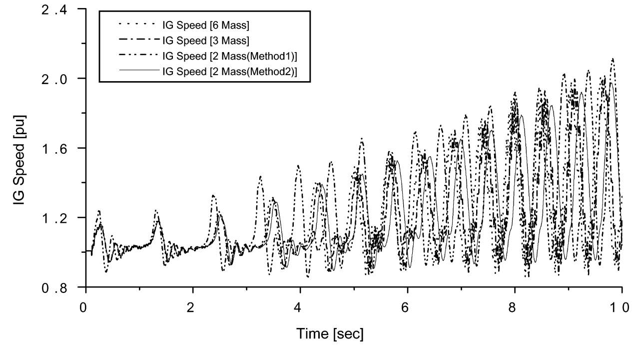

Fig. 9 *Effect of inertia constant on generator speed (condition 2, 3LG, model system-I)*

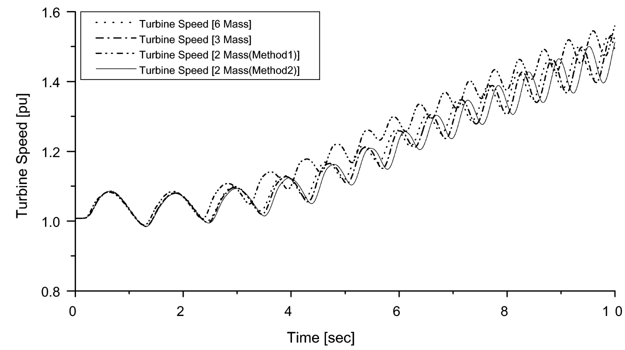

Fig. 10 *Effect of inertia constant on turbine speed (condition 2, 3LG, model system-I)*

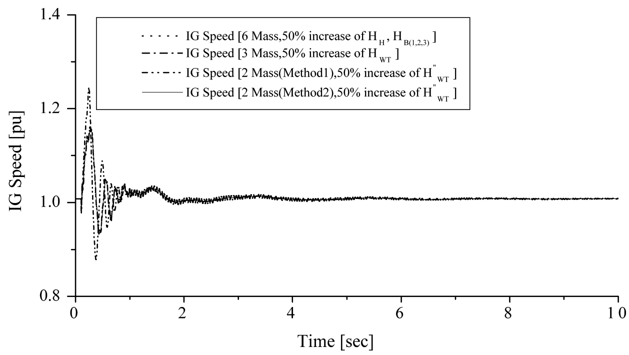

Fig. 11 *Effect of increased inertia constant of turbine on generator speed (condition 2, 3LG, model system-I)*

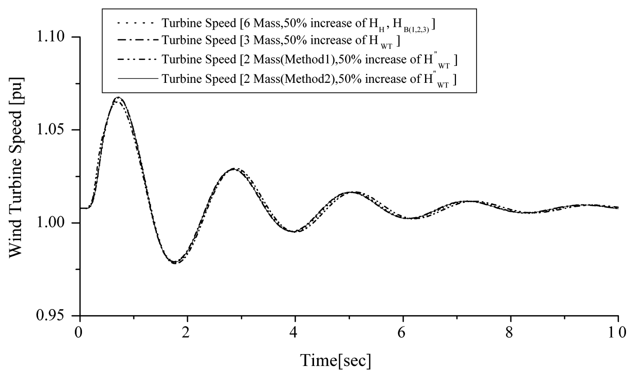

Fig. 12 *Effect of increased inertia constant of turbine on generator speed (condition 2, 3LG, model system-I)*

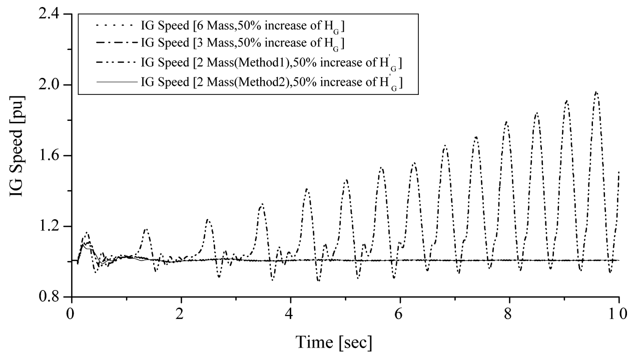

Fig. 13 *Effect of increased inertia constant of generator on its rotor speed (condition 2, 3LG, model system-I)*

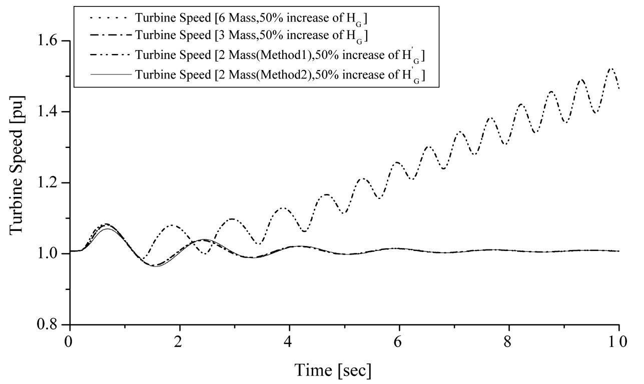

Fig. 14 *Effect of increased inertia constant of generator on turbine speed (condition 2, 3LG, model system-I)*

in Section 10. In Figs. 13 and 14, the IG rotor and turbine speeds are shown where the generator inertia constant of each drive train model is increased by about 50% from the original value shown in Section 10. It is clear from Figs. 13 and 14 that the transformation from three-mass to two-mass is needed to perform according to method2 of Fig. 2*d*; that is, gearbox and generator masses should be added together as they are separated with comparatively lower shaft stiffness. Moreover, it is seen that the increase of turbine and generator inertia constants enhances the transient stability of WTGS for all types of drive train models. From Figs. 9 to 14, it is clear that if a proper transformation process is applied, then the two-mass shaft model shows almost the same transient characteristics as those of six-mass and three-mass drive train models.

5.1.2 Effect of spring constants: In this section, the effect of spring constant on the transient stability of WTGS is demonstrated using six-mass, three-mass and two-mass drive train models. Here the dampings are neglected. A 3LG fault is considered to occur at point F of Fig. 3. First, the results of transient characteristics of six-mass drive train model are presented where the stiffness between hub–blades, gearbox–generator and hub–gearbox are increased by certain percentages from the original values as shown in Figs. 15, 16 and 17, respectively. It is seen from those figures that the stiffness between hub–blades and gearbox–generator has negligible effect on the transient stability of WTGS. But the transient stability strongly depends on the spring constant between hub and generator. In the three-mass drive train model it is also seen that the spring constant between gearbox and generator has almost no effect on the stability as shown in Fig. 18.

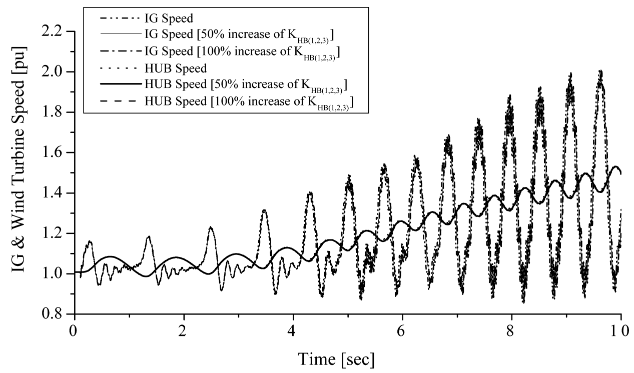

Fig. 15 *Effect of spring constant between hub and blades of six-mass model (condition 2, 3LG, model system-I)*

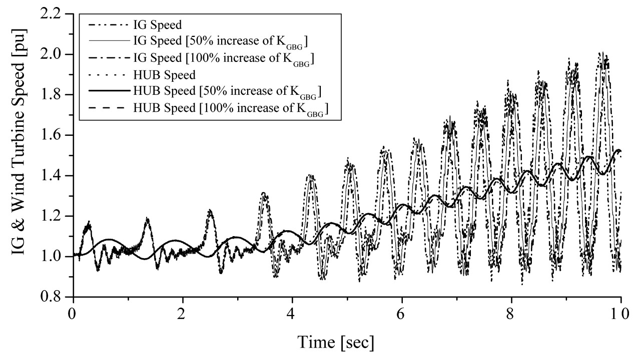

Fig. 16 *Effect of spring constant between gearbox and generator of six-mass model (condition 2, 3LG, model system-I)*

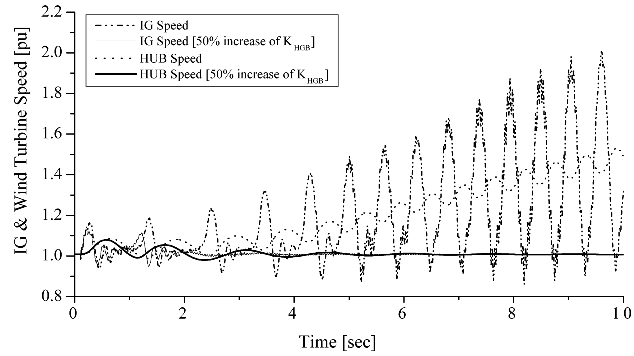

Fig. 17 *Effect of spring constant between hub and gearbox of six-mass model (condition 2, 3LG, model system-I)*

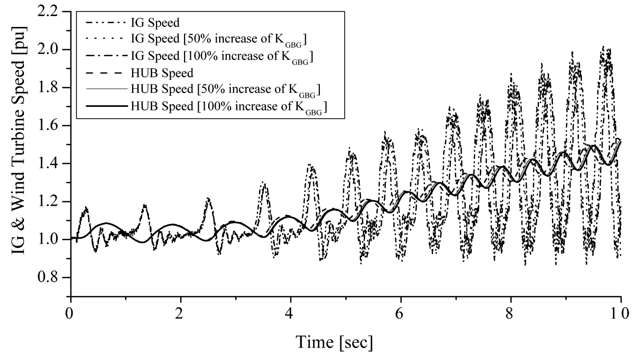

Fig. 18 *Effect of spring constant between gearbox and generator of three-mass model (condition 2, 3LG, model system-I)*

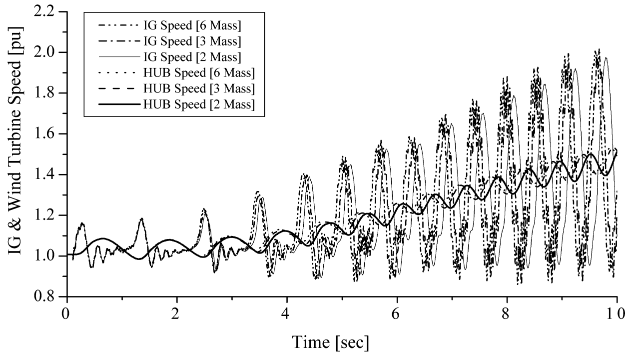

Fig. 19 *Effect of spring constant between hub and gearbox of six-, three- and two-mass models (condition 2, 3LG, model system-I)*

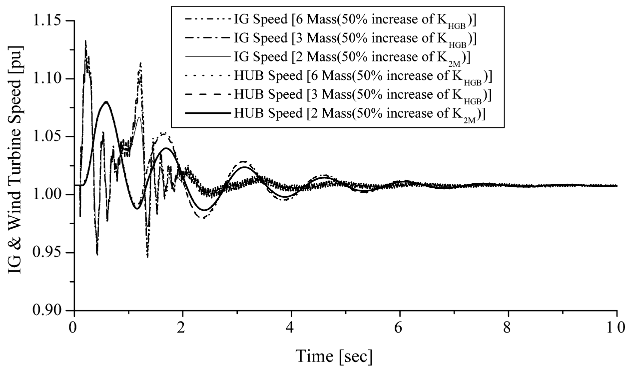

Fig. 20 *Effect of increased spring constant between hub and gearbox of six-, three- and two-mass models (condition 2, 3LG, model system-I)*

Finally, the effect of the spring constant between hub and gearbox for six-mass and three-mass models and the effect of the equivalent stiffness of a two-mass model are compared when a severe network disturbance occurs in the model system as shown in Fig. 19. Moreover, these stiffnesses are increased by 50% from the original values and their effects are observed as shown in Fig. 20. It is clear from Figs. 19 and 20 that the two-mass shaft model shows almost the same transient characteristics as those of six-mass and three-mass drive train models under network disturbance.

5.1.3 Effect of damping constants: In this section, the effect of self- and mutual-dampings of the drive train are analysed using six-mass, three-mass and two-mass models when a severe network disturbance occurs in the model system. Responses of the IG rotor and turbine speeds of the six-mass model are shown in Figs. 21 and 22, respectively, where the dampings are considered or disregarded. It is seen that both self- and mutual-dampings have significant effect on the transient stability of WTGS, and between these two dampings, the mutual damping makes the WTGS transiently more stable. But in the three-mass model, it is not possible to consider the mutual dampings between hub and blades. In the case of two-mass model, only the mutual damping between hub and gearbox is present. External damping elements represent the torque losses. As generator and gearbox masses are lumped together in the two-mass model, the self-damping of the individual elements are also lumped together. Finally, simulations have been carried out by using the damping values shown

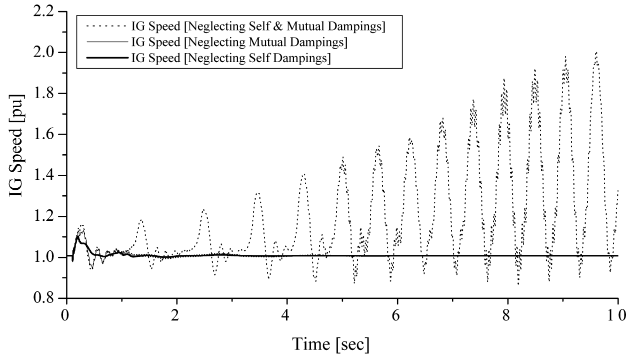

Fig. 21 *Effect of damping constant on generator speed for six-mass model (condition 2, 3LG, model system-I)*

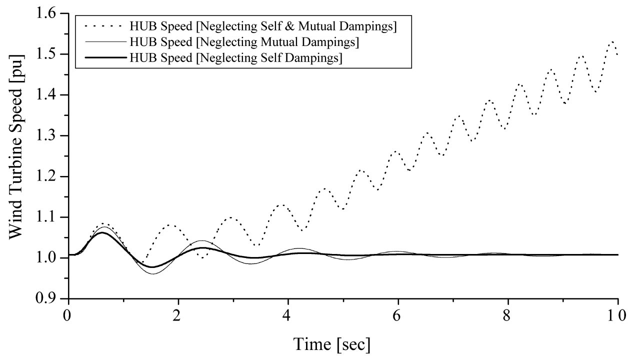

Fig. 22 *Effect of damping constant on turbine speed for six-mass model (condition 2, 3LG, model system-I)*

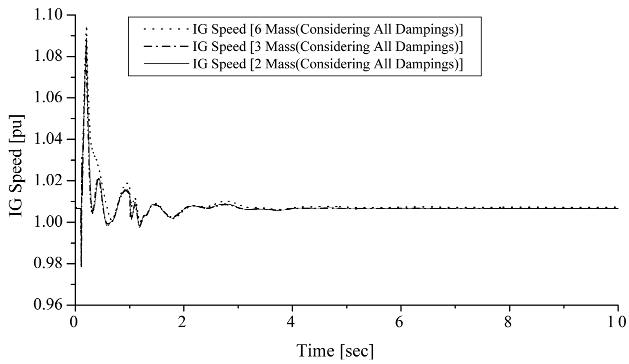

Fig. 23 *Effect of damping constant on generator speed for six-, three- and two-mass models (condition 2, 3LG, model system-I)*

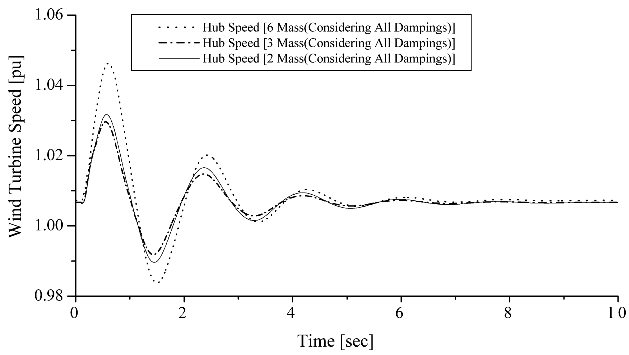

Fig. 24 *Effect of damping constant on turbine speed for six-, three- and two-mass models (condition 2, 3LG, model system-I)*

Table 4: Transient stability results for two-mass, three-mass and six-mass models (neglecting all types of dampings)

IG power (MW)	1LG fault			2LG fault			2LG fault			3LG fault		
	2M	3M	6M	2M	3M	6M	2M	3M	6M	2M	3M	6M
50	O	O	O	O	O	O	×	×	×	×	×	×
44	O	O	O	O	O	O	×	×	×	×	×	×
43	O	O	O	O	O	O	O	O	O	×	×	×
40	O	O	O	O	O	O	O	O	O	×	×	×
39	O	O	O	O	O	O	O	O	O	O	O	O

Table 5: Transient stability results for two-mass, three-mass and six-mass models (considering all types of dampings, condition 3)

IG power (MW)	1LG fault			2LS fault			2LG fault			3LG fault		
	2M	3M	6M	2M	3M	6M	2M	3M	6M	2M	3M	6M
50	O	O	O	O	O	O	O	O	O	O	O	O

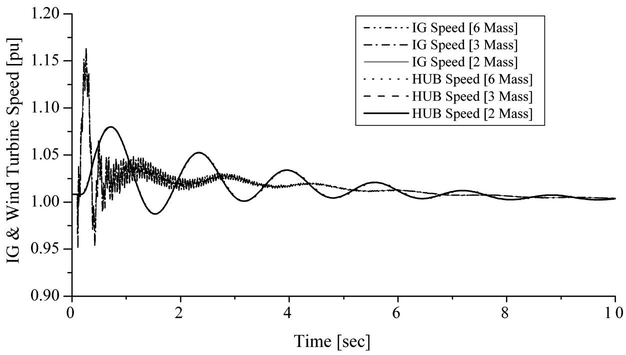

Fig. 25 *Transient effect of six-, three- and two-mass models (condition 4, 3LG, model system-II)*

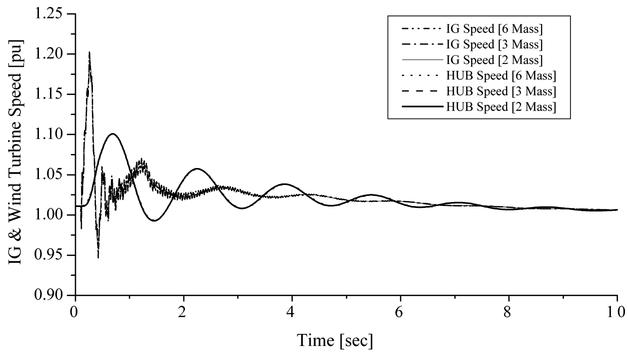

Fig. 27 *Transient effect of six-, three-, and two-mass models (condition 4, 2LG, model system-II, transformer grounded)*

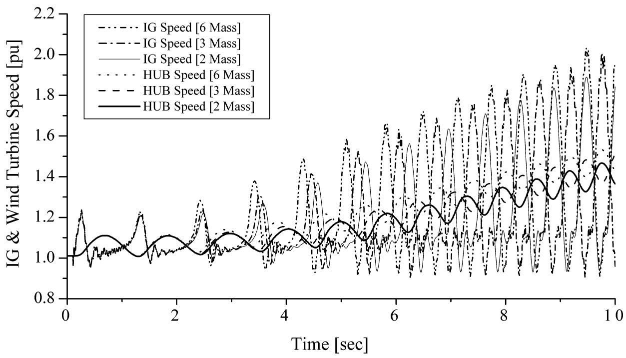

Fig. 26 *Transient effect of six-, three- and two-mass models (condition 5, 3LG, model system-II)*

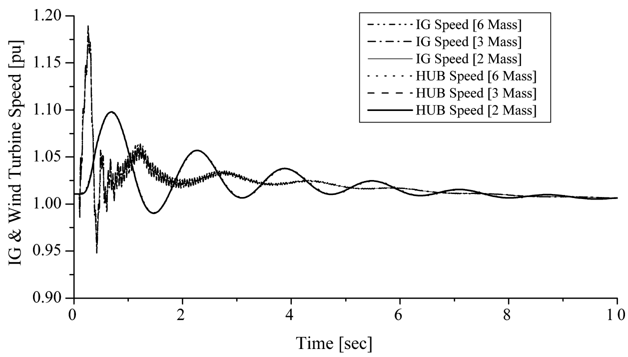

Fig. 28 *Transient effect of six-, three- and two-mass models (condition 4, 2LG, model system-II, transformer ungrounded)*

in Section 10 and it is found that the two-mass, three-mass and six-mass drive train models give almost the same results as shown in Figs. 23 and 24.

5.2 Fault analysis

The transient stability of WTGS are also analysed using the six-mass, three-mass and two-mass drive train models against different types of symmetrical and unsymmetrical fault in model system-I. Drive train parameters are taken from Section 10. The initial values at different IG output power levels can be obtained from the method described in [7]. The simulation results are shown briefly in Tables 4 and 5, with and without considering the dampings, where O and represent stable and unstable situations of WTGS, respectively. It is clear from the simulation results that in all cases two-mass shaft model gives the same transient responses as those of three-mass and six-mass drive train models.

6 Comparison using model system-II

In model system-II, longer fault clearing time and CB reclosing time are used. A fault occurs at 0.1 s, the CB on the faulted line are opened at 0.22 s and reclosed at 1.22 s. Table 3 shows the initial values used in the simulation. When a 3LG fault occurs at fault point F of Fig. 6, all types of drive train models show the similar characteristics both for condition 4 and condition 5, as shown in Figs. 25 and 26, respectively. Therefore it is clear that the three drive train models show the similar transient characteristic for both stable and unstable conditions of WTGS. Some other simulation results are presented in Figs. 27 and 28 for 2LG fault by using condition 4, where the transformer near the IG is grounded or ungrounded, respectively. In these results, the six-, three-, and two-mass drive train models also show the same transient characteristics during the network disturbance.

7 Conclusions

In this work, the transient stability of WTGS is analysed using the six-mass, three-mass and two-mass drive train models for severe network disturbance in two different types of power system models. A detailed transformation methodology from the six-mass to two-mass drive train models is presented, which can be used in the simulation analysis with reasonable accuracy. By using the transformation procedure, the inertia constants, spring constants, self-dampings of individual masses and mutual-dampings of adjacent masses of the six-mass drive train model can be converted to reduced order models. The effects of drive train parameters such as inertia constants, spring constants and damping constants are examined for the above mentioned three-types of drive train models. Moreover, different types of symmetrical and asymmetrical faults are analysed at different power levels of IG, with or without considering damping constants of six-mass, three-mass and two-mass models. Considering all the simulation results, it can be concluded that the WTGS can be expressed by the simple two-mass shaft model with reasonable accuracy and that this model is suitable for the transient stability analysis of grid connected WTGS.

8 Acknowledgment

The authors acknowledge contributions from Stavros Papathanassiou (National Technical University of Athens (NTUA)) and Dharshana Muthumuni (Manitoba HVDC Research Centre) for technical data and turbine modelling.

9 References

1 The European Wind Energy Association: 'Wind force 12—a blueprint to achieve 12% of the World's electricity from wind power by 2020'. EWEA Publications, 2005 [Online] http://www.ewea.org/

2 Souza, C.L., Neto, L.M., Guimaraes, G.C., and Moraes, A.J.: 'Power system transient stability analysis including synchronous and induction generator'. IEEE Porto Power Tech. Proc., 2001, vol. 2, p. 6

3 Tamura, J., Yamajaki, T., Ueno, M., Matsumura, Y., and Kimoto, S.: 'Transient stability simulation of power system including wind generator by PSCAD/EMTDC'. IEEE Porto Power Tech Proc., 2001, vol. 4, EMT-108

4 Abdin, E.S., and Xu, W.: 'Control design and dynamic performance analysis of a wind turbine induction generator unit', *IEEE Trans. Energy Convers.*, 2000, **15**, (1), p. 91

5 Zubia, I., Ostolaza, X., Tapia, G., Tapia, A., and Saenz, J.R.: 'Electrical fault simulation and dynamic response of a wind farm'. Proc. IASTED Int. Conf. on Power and Energy System, No.337-095, 2001, p. 595

6 Tamura, J., Yamazaki, T., Takahashi, R., Yonaga, S., Kubo, H. *et al.*: 'Analysis of transient stability of wind generators'. Conf. Record of ICEM 2002, No.148, 2002

7 Muyeen, S.M., Hasan Ali, Md., Takahashi, R., Murata, T., and Tamura, J.: 'Transient stability enhancement of wind generator by a new logical pitch controller', *IEEJ Trans. Power Energy*, 2006, **126-B**, (8), pp. 742–752

8 Hinrichsen, E.N., and Nolan, P.J.: 'Dynamics and stability of wind turbine generators', *IEEE Trans. Power Appar. Syst.*, 1982, **101**, (8), p. 2640

9 Muyeen, S.M., Hasan Ali, Md., Takahashi, R., Murata, T.,Tamura, J. *et al.*: 'Transient stability analysis of wind generator system with the consideration of multi-mass shaft model'. Int. Conf. on Power Electronics and Drive Systems (IEEE PEDS 2005), Conference CDROM, Malaysia, 2005, pp. 511–516

10 Tamura, J., Shima, Y., Takahashi, R., Murata, T., Tomaki, Y. *et al.*: 'Transient stability analysis of wind generator during short circuit faults'. Proc. Third IEEE Int. Conf. on Systems, Signals and Devices (SSD'05), 2005

11 Gonzalez Rodriguez, A.G., Burgos Payan, M., and Izquierdo Mitchell, C.: 'PSCAD based simulation of the connection of a wind generator to the network'. IEEE Porto Power Tech Proc., DRS3-307, 2001

12 Carrillo, C., Feijoo, A.E., Cidras, J., and Gonzalez, J.: 'Power fluctuations in an isolated wind plant', *IEEE Trans. Energy Convers.*, 2004, **19**, (1), p. 217

13 Petru, T., and Thiringer, T.: 'Modeling of wind turbines for power system studies', *IEEE Trans. Power Syst.*, 2002, **7**, (4), pp. 1132–1139

14 Akhmatov, V., Knudsen, H., Nielsen, A.H., Pedersen, J.K., and Poulsen, N.K.: 'Modelling and transient stability of large wind farms', *Int. J. Electr. Power Energy Syst.*, 2003, **25**, pp. 123–144

15 Akhmatov, V., Knudsen, H., and Nielsen, A.H.: 'Advanced simulation of windmills in the electric power supply', *Int. J. Electr. Power Energy Syst.*, 2000, **22**, pp. 421–434

16 Salman, S.K. *et al.*: 'Improvement of fault clearing time of wind farm using reactive power compensation'. IEEE Porto Power Tech Proc., SSR2-097, 2001

17 Salman, S.K., and Teo, A.L.J.: 'Investigation into the estimation of the critical clearing time of a grid connected wind power based embedded generator'. Proc. IEEE/PES T & D Conf. and Exhibition, 2002, Asia Pacific, vol. II, p. 975

18 Salman, S.K., and Teo, A.L.J.: 'Windmill modeling consideration and factors influencing the stability of a grid-connected wind power-based embedded generator', *IEEE Trans. Power Syst.*, 2003, **18**, (2), pp. 793–802

19 Muyeen, S.M., Hasan Ali, Md., Takahashi, R., Murata, T., and Tamura, J.: 'Transient stability analysis of grid connected wind turbine generator system considering multi-mass shaft modeling', *Electr. Power Compon. Syst.*, 2006, **34**, (10), pp. 1121–1138

20 Trudnowski, D.J., Gentile, A., Khan, J.M., and Petritz, E.M.: 'Fixed-speed wind-generator and wind-park modeling for transient stability studies', *IEEE Trans. Power Syst.*, 2004, **19**, (4), pp. 1911–1917

21 Leithead, W.E., and Connor, B.: 'Control of variable speed wind turbines: dynamic models', *Int. J. Control*, 2000, **73**, (13), pp. 1173–1188

22 Mihet-Popa, L., Blaabjerg, F., and Boldea, I.: 'Wind turbine generator modeling and simulation where rotational speed is the controlled variable', *IEEE Trans. Ind. Appl.*, 2004, **40**, (1), pp. 3–10

23 Thiringer, T.: 'Power quality measurements performed on a low-voltage grid equipped with two wind turbines', *IEEE Trans. Energy Convers.*, 1996, **11**, (3), pp. 601–606

24 Papathanassiou, S.A., and Papadopoulos, M.P.: 'Mechanical stresses in fixed speed wind turbines due to network disturbances', *IEEE Trans. Energy Convers.*, 2001, **16**, (4), pp. 361–367

25 Muyeen, S.M., Hasan Ali, Md., Takahashi, R., Murata, T., Tamura, J., Tomaki, Y., Sakahara, A., and Sasano, E.: 'Transient stability analysis of wind generator by using six-mass drive train model'. The 2006 Int. Conf. on Electrical Machines and Systems (ICEMS 2006), Session No. DS4F4-02, Ref. No. 00082, Nagasaki, Japan, November 2006

26 Heier, S.: 'Grid integration of wind energy conversion system' (John Wiley & Sons Ltd, Chichester, UK, 1998)

27 Anderson, P.M., and Bose, A.: 'Stability simulation of wind turbine systems', *IEEE Trans. Power Appar. Syst.*, 1983, **102**, (12), pp. 3791–3795

28 Resnick, R., and Halliday, D.: 'Physics for students of science and engineering—Part-I' (John Wiley & Sons, Inc., May 1961)

29 Church, A.H.: 'Mechanical vibrations' (John Wiley & Sons, Inc., September 1957)

30 Morrill, B.: 'Mechanical vibrations' (The Ronald Press Company, New York, February 1957)

31 Working Group on Prime Mover and Energy Supply Models for System Dynamic Performance Studies: 'Dynamic models for fossil fuelled steam units on power system studies', *IEEE Trans. Power Syst.*, 1991, **6**, (2), pp. 753–761

32 IEEE: Recommended practice for excitation system models for power system stability studies 'IEEE Std. 421.5', 1992

33 PSCAD/EMTDC Manual, Manitoba HVDC Research Center, 1994

34 Papathanassiou, S.A.: 'Contribution to the analysis of variable speed wind turbines with induction generator for the selection of their electrical scheme', PhD thesis, National Technical University of Athens (NTUIA), 1997

10 Appendix

The six-mass and three-mass drive train parameters in per unit (from [34]) based on high speed rotation are as follows

	6M	3M		6M	3M		6M	3M
$H_{B(1,2,3)}$	0.6388	–	K_{HGB}	54.75	54.75	D_G	0.01	0.01
H_H	0.0114	–	K_{GBG}	1834.1	1834.1	$d_{HB(1,2,3)}$	12.0	–
H_{WT}	–	1.9277	$D_{B(1,2,3)}$	0.004	–	d_{HGB}	3.5	3.5
H_{GB}	0.0806	0.0806	D_H	0.01	–	d_{GBG}	10.0	10.0
H_G	0.1419	0.1419	D_{WT}	–	0.022			
$K_{HB(1,2,3)}$	1259.8	–	D_{GB}	0.022	0.022			

The transformed two-mass data are as follows:

2M					
H''_{WT}	1.9277	K_{2M}	53.16	D'_G	0.032
H''_G	0.2225	D''_{WT}	0.022	d''_{2M}	3.5